

Cite this: DOI: 10.1039/c2dt32823b

N-alkyl functionalised expanded ring *N*-heterocyclic carbene complexes of rhodium(i) and iridium(i): structural investigations and preliminary catalytic evaluation†

Jay J. Dunsford,^{‡a} Dorette S. Tromp,^b Kingsley J. Cavell,^{*a} Cornelis J. Elsevier^b and Benson M. Kariuki^a

A series of new *N*-alkyl functionalised 6- and 7-membered expanded ring *N*-heterocyclic carbene (NHC) pro-ligands **3–6** and their corresponding complexes of rhodium(i) and iridium(i), [M(NHC)(COD)Cl] **7–14** and [M(NHC)(CO)₂Cl] **15–22** are described. The complexes have been characterised by ¹H and ¹³C{¹H} NMR, mass spectrometry, IR and X-ray diffraction. It is noted from X-ray diffraction studies that the *N*-alkyl substituents are found to orientate themselves away from the metal centre due to unfavourable steric interactions resulting in low percent buried volume (%*V*_{bur}) values in the solid state. The heterocycle ring size is also found to dictate the spatial orientation of the *N*-alkyl substituents in the neopentyl functionalised derivatives **10** and **14**. The 7-membered derivative **14** allows for a conformational 'twist' of the heterocycle ring with the *N*-alkyl substituents adopting a mutually *trans* configuration with respect to each other, while the more rigid 6-membered system **10** does not allow for this conformational 'twist' and consequently the *N*-alkyl substituents adopt a mutually *cis* configuration. The σ -donor function of this new class of expanded ring NHC ligand has also been probed by measured IR stretching frequencies of the [M(NHC)(CO)₂Cl] complexes **15–22**. A preliminary catalytic survey of the hydrogenation of functionalised alkenes with molecular hydrogen under mild conditions has also been undertaken with complex **10**, affording an insight into the application of large ring NHC ancillary ligands bearing *N*-alkyl substituents in hydrogenation transformations.

Received 26th November 2012,
Accepted 18th December 2012

DOI: 10.1039/c2dt32823b

www.rsc.org/dalton

1. Introduction

N-heterocyclic carbene (NHC) ligands have become increasingly popular in both organometallic chemistry and homogeneous catalysis over the past 20 years,¹ in part due to their readily tunable steric and electronic parameters.² To date there has been a plethora of literature reports detailing an extremely wide and diverse range of NHC ligand architectures, metal complexes and their catalytic application in the vast majority

of important transition metal mediated transformations.³ More recently our group and others have detailed the synthesis of a range of novel expanded ring NHC ligand architectures (to date there have been examples of 6-, 7- and 8-membered ring systems)⁴ and their corresponding complexes with an array of late transition metals (Ag,⁵ Rh,⁶ Ir,⁷ Pt,⁸ Pd,⁹ Ni,¹⁰ Cu,¹¹ Au¹² and Ru¹³). The application of complexes bearing expanded ring NHC ancillary ligands in catalytic transformations such as transfer hydrogenation^{6f,7} and hydrogenation,^{6c} hydrosilylation,^{8a,b} C–C cross coupling^{9c,d} and the hydration of alkynes,^{12a,b} have thus far demonstrated a number of encouraging results and in some cases novel reactivity by comparison to traditional imidazolium based analogues.^{9c} With these previous investigations in mind we are interested in further understanding the novel reactivity and scope of such expanded ring NHC complexes through modulation of both σ -donor function and the steric impact of the *N*-substituents.

Early studies in the area by Buchmeiser and co-workers detailed the synthesis of a 6-membered expanded ring NHC ligand bearing *N*-alkyl substituents (iPr) and its coordination

^aSchool of Chemistry, Main Building, Cardiff University, Cardiff, CF10 3AT Wales, UK. E-mail: cavellkj@cf.ac.uk; Fax: (+44) 029-20874030; Tel: (+44) 029-20879316

^bMolecular Inorganic Chemistry, Van't Hoff Institute for Molecular Sciences, University of Amsterdam, Science Park 904, Postbus 94157, 1090 GD Amsterdam, The Netherlands. E-mail: c.j.elsevier@uva.nl

†Electronic supplementary information (ESI) available: Structure refinement details for compounds **4**, **5**, **6**, **10** and **14**. CCDC 905711–905715. For ESI and crystallographic data in CIF or other electronic format see DOI: 10.1039/c2dt32823b

‡Present Address: School of Chemistry, University Park, University of Nottingham, Nottingham, NG7 2RD, UK.

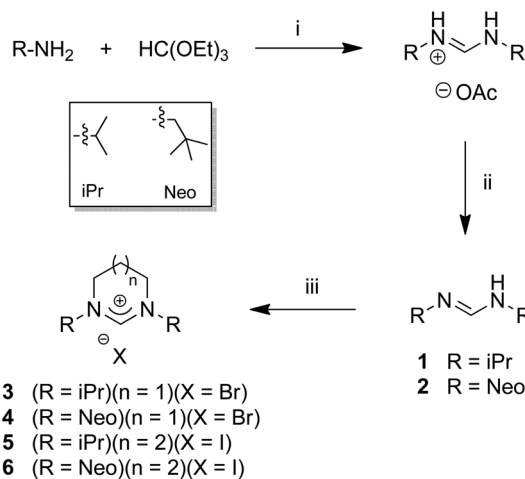
chemistry with rhodium and palladium.¹⁴ There has also been a previous example of a fused 7-membered ligand scaffold based around a biphenyl backbone bearing neopentyl (Neo) *N*-alkyl substituents detailed by Stahl and co-workers.^{9a} Following these reports, and our earlier investigations on saturated expanded ring NHCs bearing *N*-aryl substituents, we became interested in the idea of tuning the steric constraint imparted by large ring NHC systems through the incorporation of less sterically imposing *N*-alkyl substituents. We were particularly interested in the influence in which the increasingly flexible nature of such substituents would impart on both the structural conformation of the heterocycle ring and the catalytic implications this may lead to. Imidazolium based *N*-alkyl functionalised NHC complexes are well known within the literature with numerous accounts of both their synthesis and application.¹⁵ Arguably the most notable example of the catalytic application of such systems comes in the form of the iridium (iii) complexes of Crabtree and co-workers consisting of a bis-chelating NHC bearing pendant neopentyl substituents.¹⁶ This set of compounds gave exceptional TOF⁻¹ values in the transfer hydrogenation of unsaturated substrates.

Herein, we present the synthesis and characterisation of new *N*-alkyl functionalised expanded ring NHC ligands, utilising a modified synthetic protocol, and their coordination to both rhodium(i) and iridium(i) precursors. Steric and electronic parameters of the resulting complexes, and preliminary catalytic behaviour in the hydrogenation of alkynes were also investigated.

2. Results and discussion

Synthesis of *N*-alkyl functionalised expanded ring NHC-HX ligands 3–6

Synthetic routes toward previously described *N*-alkyl functionalised expanded ring NHC pro-ligands have been based around the functionalisation of a diamine backbone prior to ring closure with an appropriate C1 building block (HC(OEt)₃^{5c} or formaldehyde¹⁴). Our preferred entry into such expanded ring NHC systems has been based around a formamidine ring closure protocol,^{5a,17} which allows for the facile modulation of both heterocycle ring size and *N*-substituents.^{5a,6b} Employment of this synthetic methodology for the synthesis of 6- and 7-membered *N*-alkyl functionalised derivatives is hampered by the limited number of *N*-alkyl functionalised formamidine species reported to date.¹⁸ Hence, we have also prepared *N*-alkyl functionalised *N,N'*-dialkylformamidines *via* a modification of a previously reported literature procedure.¹⁹ In this approach utilisation of 1 equivalent of acetic acid (as apposed to a catalytic amount) affords the corresponding *N,N'*-dialkylformamidine salt, which is followed by a neutralisation step enabling the isolation of *N,N'*-dialkylformamidines **1** and **2** as stable, white crystalline solids in good yields of 82 and 89%, respectively (Scheme 1). Ring closure of the stable *N,N'*-dialkylformamidines **1** and **2** yields both 6- and 7-membered *N*-alkyl



Scheme 1 Modified synthesis of *N*-alkyl functionalised formamidines **1** and **2** and expanded ring NHC-HX pro-ligands **3–6**. (i) Amine (2 eq.), triethylorthoformate (1 eq.), acetic acid (1 eq.), 140 °C, 17 h. (ii) NaOH(aq) (1.1 eq.), Et₂O, 2 h. (iii) dihalide (1.4 eq.), K₂CO₃ (0.5 eq.), MeCN, 70 °C, 17 h.

Table 1 ¹H and ¹³C{¹H} NMR data for *N*-CH-*N* shifts of NHC-HX salts **3–6**^a

Compound	¹ H NMR shift	¹³ C{ ¹ H} NMR shift
3	8.21	149.9
4	7.89	156.2
5	7.92	155.6
6	8.94	160.4

^a Values given in ppm, measured in CDCl₃ at 400 MHz (¹H) and 125 MHz (¹³C{¹H}).

functionalised expanded ring NHC-HX pro-ligands **3–6** in yields ranging from 54 to 73% (Scheme 1).

Analysis of the *N*-alkyl functionalised NHC-HX pro-ligands **3–6** by ¹H NMR demonstrates an interesting feature. In previously reported expanded ring NHC-HX systems bearing *N*-aryl substituents, a trend in upfield shift of the NCHN proton resonance is observed with increasing heterocycle ring size.^{4b} While this remains the case regarding the isopropyl (iPr) functionalised derivatives **3** and **5** (8.21 ppm and 7.92 ppm, respectively), the neopentyl (Neo) analogues **4** and **6** demonstrate a reverse trend (7.89 ppm and 8.94 ppm, respectively) (Table 1). This implies the NCHN proton of **6** is more acidic than that of its 6-membered analogue **4**, indicative of a weaker conjugate base.²⁰ However, analysis by ¹³C{¹H} NMR reveals that the NCHN carbon demonstrates a downfield shift with increasing heterocycle ring size in both cases, in agreement with previous reports (Table 1). This novel observation may be derived from the increasingly flexible nature of the both the 7-membered heterocycle and the neopentyl *N*-alkyl substituents.

Crystals suitable for X-ray diffraction were grown by the slow diffusion of diethyl ether into a concentrated dichloromethane solution at ambient temperature. Analysis of the neopentyl functionalised compounds **4** and **6**, showed the *N*-alkyl

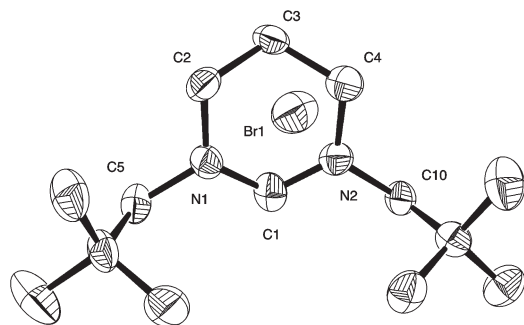


Fig. 1 ORTEP²¹ ellipsoid plot at 50% probability of the molecular structure of **4**. Hydrogens and solvent molecules have been omitted for clarity. Selected bond lengths (Å) and angles (°) for 6-Neo-HBr: C(1)–N(1), 1.327(8); C(1)–N(2), 1.325(8); N(1)–C(2), 1.477(8); N(2)–C(4), 1.456(9); N(1)–C(5), 1.475(9); N(2)–C(10), 1.470(9); N(1)–C(1)–N(2), 122.7(7); C(1)–N(1)–C(2), 121.6(6); C(1)–N(2)–C(4), 121.6(6); C(1)–N(1)–C(5), 118.9(6); C(1)–N(2)–C(10), 117.8(6).

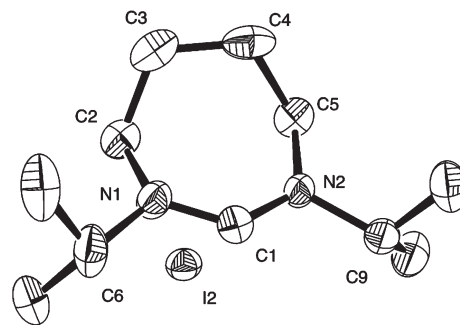


Fig. 3 ORTEP²¹ ellipsoid plot at 50% probability of the molecular structure of **5**. Hydrogens and solvent molecules have been omitted for clarity. Selected bond lengths (Å) and angles (°) for 7-iPr-HI: C(1)–N(1), 1.316(18); C(1)–N(2), 1.310(17); N(1)–C(2), 1.476(18); N(2)–C(5), 1.433(18); N(1)–C(6), 1.471(18); N(2)–C(9), 1.483(16); N(1)–C(1)–N(2), 130.2; C(1)–N(1)–C(2), 121.8(16); C(1)–N(2)–C(5), 125.3(16); C(1)–N(1)–C(6), 118.5(13); C(1)–N(2)–C(9), 116.9(13).

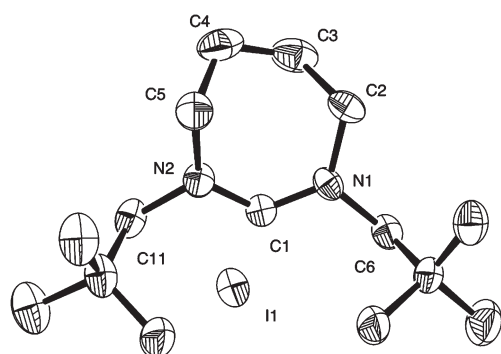


Fig. 2 ORTEP²¹ ellipsoid plot at 50% probability of the molecular structure of **6**. Hydrogens and solvent molecules have been omitted for clarity. Selected bond lengths (Å) and angles (°) for 7-Neo-HI: C(1)–N(1), 1.326(6); C(1)–N(2), 1.324(6); N(1)–C(2), 1.480(7); N(2)–C(5), 1.475(7); N(1)–C(6), 1.469(7); N(2)–C(11), 1.474(7); N(1)–C(1)–N(2), 127.4(5); C(1)–N(1)–C(2), 125.0(4); C(1)–N(2)–C(5), 123.4(4); C(1)–N(1)–C(6), 116.3(4); C(1)–N(2)–C(11), 117.7(4).

Table 2 Selected bond lengths (Å) and angles (°) for NHC-HX ligands **4**, **5**, and **6**

	4	5	6
C(1)–N(1)	1.327(8)	1.316(18)	1.326(6)
C(1)–N(2)	1.325(8)	1.310(17)	1.324(6)
N(1)–C(alkyl)	1.475(9)	1.471(18)	1.469(7)
N(2)–C(alkyl)	1.470(9)	1.483(16)	1.474(7)
N(1)–C(1)–N(2)	122.7(7)	130.2	127.4(5)
N(1)–C(1)–C(alkyl)	118.9(6)	118.5(13)	116.3(4)
N(2)–C(1)–C(alkyl)	117.8(6)	116.9(13)	117.7(4)

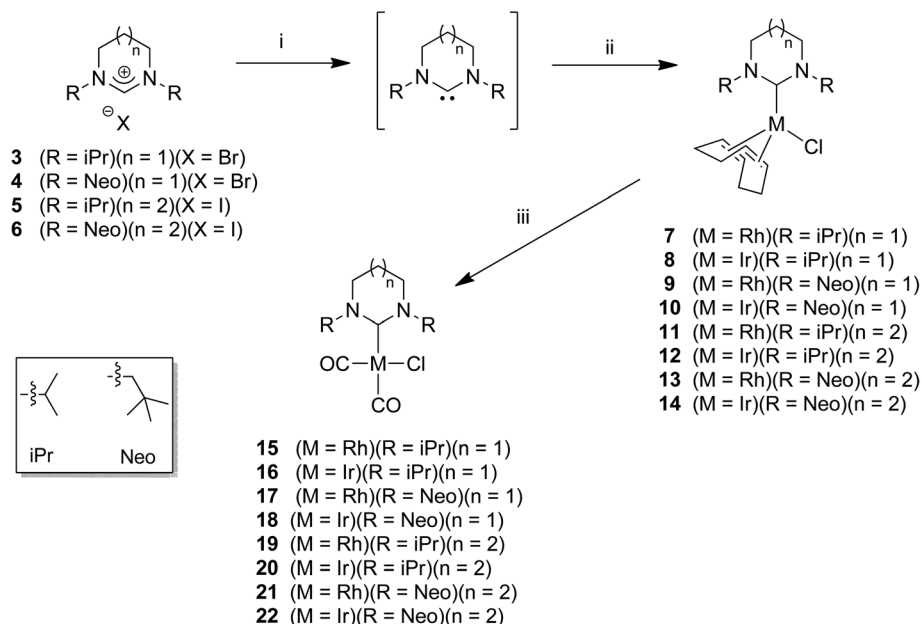
substituents to be mutually *cis* to each other with the bulky terminal *tert*-butyl groups serving to effectively block one side of the ligand coordination sphere (Fig. 1 and 2). However, this observation may not be representative of the solution state conformation with free rotation enabled about the NCH₂C(CH₃)₃ bond. In analysis of the N–C_{NHC}–N bond angles, ligands **4** and **6** increase with increasing ring size from 6- to 7-membered derivatives, with values of 122.7(7)° and 127.4(5)°,

respectively (Table 2). This observation is consistent with previously reported data for related *N*-aryl functionalised expanded ring NHC systems.^{5a} Through modulation of the *N*-alkyl substituents to isopropyl in **5** (Fig. 3) the N–C_{NHC}–N bond angle is observed to increase further still to 130.2°. To the best of our knowledge this represents the largest N–C_{NHC}–N bond angle reported to date for any NHC–HX salt and even rivals those of previously reported acyclic diaminocarbene systems.²² It is also noteworthy to mention that all measured N–C_{NHC}–N bond angles of the *N*-alkyl functionalised systems are found to be greater than those of their related 6- and 7-membered *N*-aryl counterparts (6-Mes-HBr 114.7(13)° and 7-Mes-HI 116.6(4)°).^{5a}

Synthesis of rhodium(i) and iridium(i) complexes

The *N*-alkyl functionalised NHC·HX amidinium salts **3–6** were coordinated to both rhodium(i) and iridium(i) precursors ([M(COD)Cl]₂) providing a comparison of physical and spectroscopic data with that of related complexes bearing *N*-aryl substituents.^{5–13} As noted previously the [Rh(6-*i*Pr)(COD)Cl] complex **7** has been reported by Buchmeiser *et al.*,¹⁴ herein we will expand upon this work through the analysis of alternate *N*-alkyl substituents (6-Neo) and larger ring NHC species (7-*i*Pr and 7-Neo). The synthesis of the rhodium(i) and iridium(i) complexes **7–14** of the general formula, [M(NHC)(COD)Cl] was achieved through the addition of *in situ* generated free carbene directly to the corresponding [M(COD)Cl]₂ dimer in THF under inert conditions, affording the desired complexes **7–14** as air stable yellow solids in yields ranging from 69 to 91% (Scheme 2).

Analysis of the ¹H NMR data for the neopentyl functionalised complexes **9**, **10**, **13** and **14**, reveals a splitting of the NCH₂C(CH₃)₃ proton resonances with two distinct signals appearing at *ca.* 5.5 and 3.4 ppm, respectively. This feature is possibly not surprising considering the degree of free rotation enabled about the NCH₂C(CH₃)₃ bond in question. The terminal *tert*-butyl groups appear as a sharp singlet corresponding to 18 protons at *ca.* 1 ppm.²³ Analysis of the ¹³C{¹H} NMR shift



Scheme 2 The synthesis of rhodium(i) and iridium(i) complexes [M(NHC)(COD)Cl] (**7–14**) and [M(NHC)(CO)₂Cl] (**15–22**). (i) KHDMS (1.4 eq.), THF (10 ml), rt, 30 min. (ii) [Rh/Ir(COD)Cl]₂ (0.5 eq.), THF (10 ml), rt, 1 h. (iii) CO_(g) (1 atm), DCM (10 ml), rt, 20 min.

of the N-C_{NHC}-N carbon of complexes **7–14** demonstrates an observable downfield shift in resonance with increasing heterocycle ring size, in line with previous observations.^{9c}

Solid-state analysis of rhodium(i) and iridium(i) complexes

Single crystals suitable for X-ray diffraction were grown by the slow vapour diffusion of diethyl ether into a concentrated dichloromethane solution of the complex in question. The conformations of the neopentyl substituents, relative to each other differ with heterocycle ring size, in contrast to their NHC·HX precursors (Fig. 1 and 2). In the 6-membered complex, **10** the *N*-alkyl substituents are observed to adopt a mutually *cis* conformation with regard to each other and a *trans* conformation in relation to the cyclooctadiene co-ligand (Fig. 4). This is in contrast to the conformation adopted in the 7-membered complex **14**, where a *trans* conformation of the *N*-alkyl substituents is favoured, facilitated by the inherent ‘twist’ of the NHC heterocycle backbone (Fig. 5). This feature is interesting in that it may have been predicted that a mutually *cis* conformation would be preferred with regard to alleviation of steric impact with the bulky cyclooctadiene co-ligand. Selected bond lengths and angles for the neopentyl functionalised iridium(i) complexes **10** and **14** are provided in Table 4. An analysis of the C_{NHC}-Ir bond lengths reveals a slight decrease with increasing heterocycle ring size from 2.085(6) to 2.050(8) Å. This observation would be expected considering the previously described relationship of σ-donor function to NHC heterocycle ring size and from the downfield shift of the N-C_{NHC}-N resonance in the ¹³C{¹H} NMR measurements (Table 3). This decrease in bond length is not always evident, for example in the related *N*-aryl functionalised systems the

steric constraint imposed by the bulky *N*-aryl substituents is often found to lead to a slight increase in bond length with increasing heterocycle ring size.^{5–13} The N-C_{NHC}-N bond angles of complexes **10** and **14** become more acute with increasing heterocycle ring size from 118.5(6)° to 114.1(7)°. This feature is unexpected in that all previous reports concerning related *N*-aryl functionalised complexes demonstrate more obtuse N-C_{NHC}-N bond angles in the transition from 6- to 7-membered derivatives.^{5–13} The observed reduction in bond angle from the 6- to 7-membered derivatives may be attributed to the ‘twist’ conformation adopted by the 7-membered heterocycle **14** as a consequence of the *trans* configuration of the neopentyl *N*-alkyl substituents (Fig. 5). Other important bond angles to consider in such complexes are the C_{NHC}-N-C_{Nalkyl} angles. These angles become more acute with increasing ring size, 120.4(6) and 120.9(6) for **10** and 118.0(7) and 118.1(7) for **14**, which is consistent with their *N*-aryl counterparts,^{5–13} although the influence these angles have upon the steric environment around the metal coordination sphere may differ from the corresponding *N*-aryl counterparts as a consequence of the increased degree of flexibility associated with the *N*-alkyl substituents.

The influence of the *N*-substituents upon the steric environment of the metal centre may be quantified by the percent buried volume (%V_{bur}) analysis.²⁵ Subjection of complexes **10** and **14** to such an analysis affords comparably low %V_{bur} values of 33.4 and 31.0, respectively (Table 4).²⁶ These low calculated values reflect the fact that the neopentyl *N*-alkyl substituents are orientated away from the metal coordination sphere as a consequence of the steric repulsion imparted by the bulky cyclooctadiene co-ligand (Fig. 4 and 5). The observed decrease

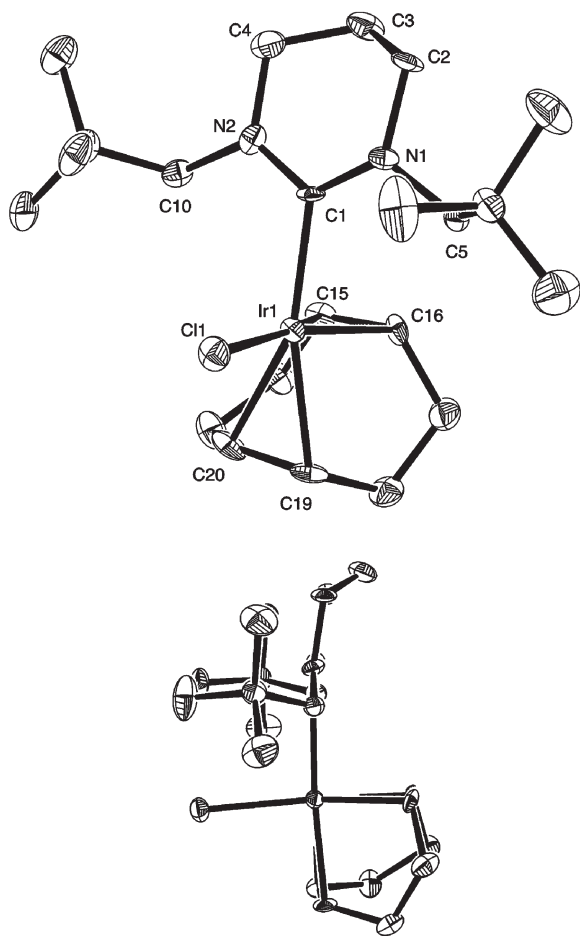


Fig. 4 ORTEP²¹ ellipsoid plot at 50% probability of the molecular structure of **10**. Hydrogens and solvent molecules have been omitted for clarity. Selected bond lengths (Å) and angles (°) for [Ir(6-Neo)(COD)Cl]: C(1)–N(1), 1.336(9); C(1)–N(2), 1.347(9); N(1)–C(5), 1.470(9); N(2)–C(10), 1.456(9); C(1)–Ir(1), 2.085(6); C(15)–Ir(1), 2.133(6); C(16)–Ir(1), 2.103(6); C(19)–Ir(1), 2.197(7); C(20)–Ir(1), 2.161(7); Ir(1)–Cl(1), 2.3783(17); C(15)–C(16), 1.423(10); C(19)–C(20), 1.388(11); N(1)–C(1)–N(2), 118.5(6); C(1)–N(1)–C(5), 115.2(6); C(1)–N(2)–C(10), 120.9(6); C(1)–Ir(1)–Cl(1), 94.14(18); C(1)–N(1)–C(2), 123.6(6); C(1)–N(2)–C(4), 123.0(6).

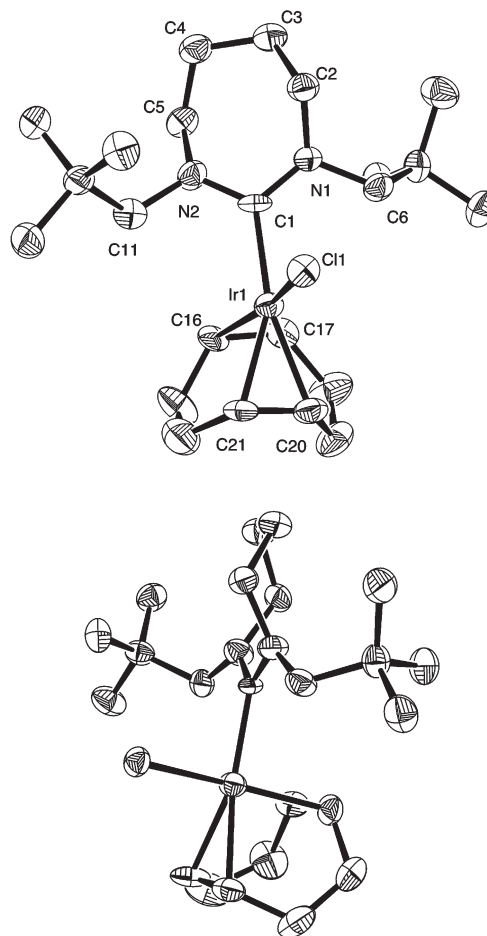


Fig. 5 ORTEP²¹ ellipsoid plot at 50% probability of the molecular structure of **14**. Solvent molecules have been omitted for clarity. Selected bond lengths (Å) and angles (°) for [Ir(7-Neo)(COD)Cl]: C(1)–N(1), 1.358(11); C(1)–N(2), 1.358(12); C(2)–N(1), 1.476(12); C(5)–N(2), 1.477(12); C(1)–Ir(1), 2.050(6); C(16)–Ir(1), 2.131(9); C(17)–Ir(1), 2.119(9); C(20)–Ir(1), 2.170(9); C(21)–Ir(1), 2.157(9); Ir(1)–Cl(1), 2.380(2); C(16)–C(17), 1.418(14); C(20)–C(21), 1.366(17); N(1)–C(1)–N(2), 114.1(7); C(1)–N(1)–C(2), 120.1(8); C(1)–N(2)–C(5), 121.7(8); C(1)–Ir(1)–Cl(1), 88.4(3); C(1)–N(1)–C(6), 118.0(7); C(1)–N(2)–C(11), 118.8(7).

in % V_{bur} value from the 6- to 7-membered derivative is again inverse to the expected trend, although possibly not surprising given the measured decrease in N–C_{NHC}–N bond angle (Table 4) and the spatial orientation adopted by the neopentyl substituents in the 7-membered derivative **14**. Again, it is important to stress that the values for the corresponding structures are calculated in the solid state and may not be representative of the solution state behaviour given the element of free rotation about the NCH₂C(CH₃)₃ bond.

Infra-red studies

In order to probe the σ -donor function of the *N*-alkyl functionalised expanded ring NHC ancillary ligands in greater detail, complexes of the general formula, [M(NHC)(CO)₂Cl] **15–22** were prepared. The complexes were accessed *via* the displacement of the cyclooctadiene co-ligand of the [M(NHC)(COD)Cl] complexes **7–14** *via* bubbling CO gas (1 atm) through a

Table 3 ¹³C{¹H} NMR N–C_{NHC}–N shifts of *N*-alkyl functionalised rhodium(i) and iridium(i) complexes **7–14**

Complex	¹³ C NMR shift (ppm) ^a
[Rh(6- <i>i</i> Pr)(COD)Cl] ¹⁴ 7	204.1 ¹⁴
[Ir(6- <i>i</i> Pr)(COD)Cl] 8	— ^b
[Rh(6-Neo)(COD)Cl] 9	208.0
[Ir(6-Neo)(COD)Cl] 10	202.2
[Rh(7- <i>i</i> Pr)(COD)Cl] 11	224.8
[Ir(7- <i>i</i> Pr)(COD)Cl] 12	209.1
[Rh(7-Neo)(COD)Cl] 13	— ^b
[Ir(7-Neo)(COD)Cl] 14	221.1

^a Measured in CDCl₃. ^b Not observed.

dichloromethane solution of the corresponding complex for 20 minutes at ambient temperature (Scheme 2).^{4b} This method for the quantification of σ -donor function of ancillary ligands

Table 4 Selected bond lengths (Å), angles (°) and percent buried volume (% V_{bur}) values for complexes **10** and **14**

	10	14
C _{NHC} -Ir	2.085(6)	2.050(8)
Ir-Cl	2.3783(17)	2.380(2)
Ir-C _{trans} Cl	2.133(6)	2.123(9)
Ir-C _{trans} NHC	2.103(6)	2.119(9)
Ir-C _{trans} NHC	2.197(7)	2.170(9)
Ir-C _{trans} NHC	2.161(7)	2.157(9)
C=C _{trans} Cl	1.423(10)	1.418(14)
C=C _{trans} NHC	1.388(11)	1.366(17)
N-C _{NHC} -N	118.5(6)	114.1(7)
C _{NHC} -Ir-Cl	94.14(18)	88.4(3)
C _{NHC} -N-C _{Nalkyl}	120.4(6)	118.0(7)
C _{NHC} -N-C _{Nalkyl}	120.9(6)	118.1(7)
% V_{bur}^a	33.4	31.0

^a Percent buried volume (% V_{bur}) calculated utilising the SambVca software.²⁴

Table 5 Measured carbonyl IR stretching frequencies for [M(NHC)(CO)₂Cl] complexes **15–22**^a

Complex	ν (CO) cm ⁻¹	ν_{av} (CO) cm ⁻¹
[Rh(6- <i>i</i> Pr)(CO) ₂ Cl] ¹⁴ 15	1982, 2063 ^b	2023 ^b
[Ir(6- <i>i</i> Pr)(CO) ₂ Cl] 16	1982, 2062	2022
[Rh(6- <i>Neo</i>)(CO) ₂ Cl] 17	1989, 2068	2029
[Ir(6- <i>Neo</i>)(CO) ₂ Cl] 18	1988, 2066	2027
[Rh(7- <i>i</i> Pr)(CO) ₂ Cl] 19	1988, 2049	2019
[Ir(7- <i>i</i> Pr)(CO) ₂ Cl] 20	1981, 2056	2019
[Rh(7- <i>Neo</i>)(CO) ₂ Cl] 21	1972, 2056	2014
[Ir(7- <i>Neo</i>)(CO) ₂ Cl] 22	1972, 2054	2013

^a Measured in CDCl₃. ^b Measured in DCM.

has been utilised extensively within the literature since the introduction of the Tolman electronic parameter (TEP).²⁷

The average carbonyl stretching frequencies of complexes **15–22** fall between 2029 and 2013 cm⁻¹ (Table 5). The 6-membered neopentyl functionalised complexes **17** and **18** demonstrate average values of 2029 and 2027 cm⁻¹ respectively, while their 7-membered analogues **21** and **22** demonstrate a shift to lower wavenumbers of 2014 and 2013, respectively. This decrease in average wave number demonstrates the increased basicity of the 7-membered ancillary ligands, in line with observations noted for their *N*-aryl counterparts.^{4b} Similar observations are noted for the isopropyl functionalised complexes **15**, **16**, **19** and **20** (Table 5). NHC ligands.^{9c} Attempting to correlate the σ -donor strength of the ancillary ligands, as measured by average carbonyl bond stretching frequencies to measured N-C_{NHC}-N bond angles^{4b} is hampered by the unusual decrease in bond angle demonstrated by complex **14** in comparison with **10**. Although there is a marked decrease in N-C_{NHC}-N bond angle, (*ca.* 4°) due to the alteration in heterocycle conformation due to the orientation adopted by the neopentyl substituents, the measured decrease in average carbonyl bond stretching frequency from **10** to **14** is still indicative of the 7-membered complex **14** being a stronger

σ -donor ligand. This observation may be due to changes in heterocycle conformation in complex **14** in the solution state. Although the solid-state structure demonstrates a *trans* configuration of the neopentyl substituents relative to each other and a 'twist' conformation of the heterocycle (Fig. 5), this may not be representative of the solution state behaviour. In the solution state with free rotation enabled about the NCH₂C-(CH₃)₃ bond, the conformation of the heterocycle may fall more in line with the related *N*-aryl complexes^{4a,b} allowing an increase in N-C_{NHC}-N bond angle.

Hydrogenation catalysis

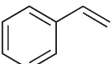
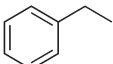
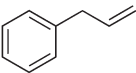
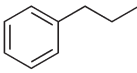
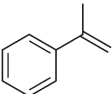
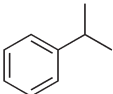
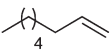
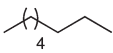
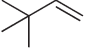
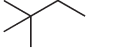
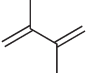
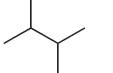
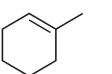
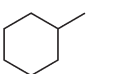
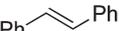
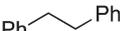
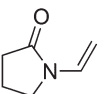
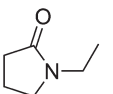
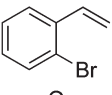
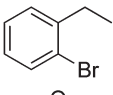
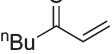
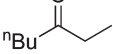
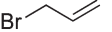
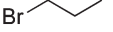
A preliminary evaluation of this class of ancillary NHC ligand in the hydrogenation of alkenes was undertaken employing the [Ir(6-*Neo*)(COD)Cl] complex **10**. Initially, styrene was investigated as a model substrate as the non-hindered nature of the terminal alkene functionality would be expected to allow the effective reduction of the double bond under relatively mild conditions (Table 6). Analysis of Table 6 shows that at relatively low catalytic loadings (0.01 mol%) the influence of the solvent employed is pronounced (Table 6, entries 1–6). The employment of primary alcohols, ethanol and methanol (entries 1 and 2) affords the quantitative conversion to ethylbenzene at ambient temperature within 1 h at 5 bar hydrogen pressure. Changing the solvent to the secondary alcohol, *i*PrOH (entry 3) leads to a pronounced reduction in overall percentage yield (40%). The employment of other common solvents also gives considerably lower overall percentage yields after 1 h at ambient temperature (entries 4–6). The parameters of time and pressure were also examined and it may be observed that in the employment of conditions identical to entry 1, complete conversion to ethylbenzene is observed in less than 30 minutes (entry 7). Reduction of the hydrogen pressure to 3

Table 6 Catalyst optimisation for the hydrogenation of styrene with [Ir(6-*Neo*)(COD)Cl], **10**^a

Entry	Solvent	<i>t</i> (min)	<i>P</i> (bar)	% Yield ^b
1	EtOH	60	5	100
2	MeOH	60	5	100
3	<i>i</i> PrOH	60	5	40
4	THF	60	5	12
5	Acetone	60	5	34
6	DCE	60	5	4
7	EtOH	30	5	100
8	EtOH	30	3	100
9	EtOH	30	1	58

^a Reaction conditions: Styrene (1 mmol), [Ir(6-*Neo*)(COD)Cl] **10** (0.01 mol%, THF stock solution), solvent (20 ml), decane (1 mmol, internal standard). ^b Percentage yields based upon consumption of substrate by GCMS.

Table 7 Substrate scope for the catalytic hydrogenation of terminal alkenes utilising [Ir(6-Neo)(COD)Cl] complex **10**^a

Entry	Substrate	Product	<i>t</i> (h)	% Yield ^b
1			0.5	100
2			0.5	100
3			1	43
4			0.5	100
5			0.5	100
6			1	52
7			16	46
8			16	>1
9			16	>1
10			1	100
11			1	69
13			1	100
14			1	100

^a Reaction conditions: Substrate (1 mmol), catalyst (0.01 mol%), THF stock solution, EtOH (20 ml), decane (1 mmol, internal standard), H₂ (5 bar). ^b Percentage yield based upon consumption of substrate by GCMS.

bar was found to have no effect on the overall catalytic activity displayed by the system although a further reduction to atmospheric pressure leads to a significant decrease to 58% conversion after 1 h (entries 8 and 9). With optimal conditions established, complex **10**, [Ir(6-Neo)(COD)Cl] was tested with a range of substituted alkene substrates (Table 7). It may be noted that similar activities to styrene are observed in the hydrogenation of allyl benzene (entry 2) although in the utilisation of the increasingly hindered α -methylstyrene, a pronounced decrease in activity is observed with a percentage conversion of 43% observed after 1 h at 5 bar hydrogen pressure. The hydrogenation of non-hindered terminal alkenes, such as 1-octene and 3,3-dimethyl-1-butene (entries 4 and 5) were also found to proceed effectively, reaching full

conversion within 1 h at 5 bar hydrogen pressure. For the sterically demanding 2,3-dimethyl-1,3-butadiene substrate, a significant decrease in activity was observed (entry 6). The overall percentage conversion after 1 h at 5 bar is found to be 52%, which is consistent with the value obtained for α -methylstyrene substrate (entry 3). No partially hydrogenated 2,3-dimethyl-1,3-butadiene could be detected. Hydrogenation of the *cis*-internal alkene cyclooctene (COE) substrate also proved challenging (46%) even after extended reaction periods of 16 h. These observations are consistent with the steric demand of the substrate. Similarly, for increasingly hindered *cis*- and *trans*-internal alkenes (entries 8 and 9) conversions after prolonged reaction times are significantly reduced with only very small yields of reduced products observed.

A preliminary study of functional group tolerance of complex **10** was also been undertaken (Table 7, entries 10–14). Terminal alkene species bearing ketone functionalities were reduced routinely in quantitative yield, without further reduction of the ketone to its corresponding alcohol (entries 10 and 13). Complex **10** was also found to tolerate halide-containing substrates (entries 11 and 14). It is interesting to note that the overall percentage yield afforded in entry 11 is 69% in comparison to the quantitative conversion achieved for the related styrene substrate (entry 1). It appears that the bromide in the *ortho*-position has a detrimental effect on the catalytic activity, possibly as a consequence of unfavourable steric interactions.

3. Conclusions

In summary, a range of new 6- and 7-membered *N*-alkyl functionalised expanded ring NHC·HX ancillary ligands have been synthesised *via* modified synthetic procedures. The ligands have been employed in the synthesis of both rhodium(i) and iridium(i) complexes of the general formula, [M(NHC)(COD)Cl]. The novel structural parameters of the complexes have been probed by solid-state analysis, affording an insight into the influence in which modulation of *N*-substituents has upon heterocycle conformation, and *N*-C_{NHC}-*N* bond angles in particular. To gain an insight into the σ -donor function of the ancillary *N*-alkyl functionalised ligands, [M(NHC)(CO)₂Cl] derivatives were prepared from their corresponding [M(NHC)(COD)Cl] complexes allowing an analysis of measured carbonyl bond stretching frequencies. A preliminary evaluation of complex **10** in the hydrogenation of unsaturated C–C containing substrates was also undertaken. This study demonstrated **10** to be effective in the reduction of non-hindered substrates under mild conditions, although employment of increasingly hindered substrates facilitated less satisfactory outcomes. Current work in our laboratory is focused upon the employment of the *N*-alkyl functionalised expanded ring NHC ancillary ligands in alternate transition metal mediated transformations, the results of which will be reported in due course.

4. Experimental

General remarks

All manipulations were performed using standard Schlenk techniques under an argon atmosphere, except where otherwise noted. All complexes after their formation were treated under aerobic conditions. Solvents of analytical grade were freshly distilled using an MBraun SPS-800 solvent purification system. Deuterated solvents for NMR measurements were distilled from the appropriate drying agents under N₂ immediately prior to use, following standard literature methods.²⁸ All commercially available reagents were used as received. NMR spectra were obtained on a Bruker Advance AMX 400 or 500. The chemical shifts are given as dimensionless δ values and are frequency referenced relative to the peak for TMS for ¹H and ¹³C. Coupling constants *J* are given in Hertz as positive values regardless of their real individual signs. The multiplicity of the signals is indicated as “s”, “d”, “t” or “m” for singlet, doublet, triplet or multiplet, respectively. High-resolution mass spectra were obtained in electrospray (ES) mode unless otherwise reported on a Waters Q-ToF micromass spectrometer. GCMS data was obtained on an Agilent Technologies 6890N GC system with an Agilent Technologies 5973 inert MS detector with MSD.

General procedure for synthesis of *N*-Alkyl formamidines

A round bottom flask was charged with the appropriate amine (60 mmol), triethylorthoformate (30 mmol) and acetic acid (30 mmol). The reaction mixture was heated to 140 °C for 17 h with stirring prior to the removal of all volatiles *in vacuo* furnishing the acetic acid salt. The acetic salt was dissolved in a minimum amount of diethyl ether and aqueous NaOH (1.1 eq.) added slowly and the mixture stirred at ambient temperature for 2 h. The organic layer was collected, the aqueous layer washed with diethyl ether (3 × 30 ml), dried over MgSO₄ and evaporated to dryness to furnish the desired formamidine species.

***N,N'*-Bis(isopropyl)formamidine (1).** White crystalline solid, yield 82% (3.15 g). ¹H NMR (CDCl₃, 400 MHz, 298 K): δ 7.26 (1H, s, NCHN), 2.29 (2H, s, NCH₂C(CH₃)₃), 0.87 (18 H, s, NCH₂C(CH₃)₃). ¹³C{¹H} NMR (CDCl₃, 125 MHz, 298 K): δ 165.0 (s, NCHN), 49.0 (s, NCH₂C(CH₃)₃), 27.1 (s, NCH₂C(CH₃)₃). MS (ESI): *m/z* 129.1395 (M⁺ + H) – C₇H₁₇N₂ requires 129.1392.

***N,N'*-Bis(2,2-dimethylpropane)formamidine (2).** White crystalline solid, yield 89% (4.91 g). ¹H NMR (CDCl₃, 400 MHz, 298 K): δ 7.38 (1H, s, NHCN), 4.07 (1H, s (broad), NH), 3.45 (2H, m, NCH(CH₃)₂), 1.11 (12H, d, ³J_{HH} = 7.2, NCH(CH₃)₂). ¹³C{¹H} NMR (CDCl₃, 125 MHz, 298 K): δ 149.1 (s, NHCN), 49.5 (s, NCH(CH₃)₂), 24.2 (s, NCH₂(CH₃)₂). MS (ESI): *m/z* 184.1936 (M⁺ + H) – C₁₁H₂₄N₂ requires 184.1939.

General procedure for synthesis of *N*-alkyl functionalised NHC·HX salts

A round bottom flask was charged with *N,N'*-bis(alkyl)formamidine (20 mmol), K₂CO₃ (10 mmol) and suspended in acetonitrile (80 ml). To this stirred solution 1,3-dibromopropane

(3 and 4) or 1,4-diiodobutane (5 and 6) (24 mmol) was added and the solution heated to reflux for 17 h. Upon cooling the solvent was removed *in vacuo* before the residue was taken up in DCM (20 ml), filtered to remove all potassium salts and recrystallised *via* the slow addition of diethyl ether yielding a white crystalline suspension isolated by filtration.

6-*i*Pr·HBr (3). White crystalline solid, yield 73% (3.64 g). ¹H NMR (CDCl₃, 400 MHz, 298 K): δ 8.12 (1H, s, NHCN); 3.94 (2H, s, NCH(CH₃)₂); 3.34 (4H, t, ³J_{HH} = 5.8 Hz, NCH₂); 1.99 (2H, q, ³J_{HH} = 5.0 Hz, NCH₂CH₂); 1.29 (12H, d, ³J_{HH} = 6.7 Hz, NCH(CH₃)₂). ¹³C{¹H} NMR (CDCl₃, 125 MHz, 298 K): δ 149.9 (s, NHCN); 56.1 (s, NCH(CH₃)₂); 38.8 (s, NCH₂); 18.9 (s, NCH(CH₃)₂); 17.9 (s, NCH₂CH₂). MS (ESI) *m/z* 169.1707 (M⁺ – I) – C₁₁H₂₃N₂ requires 169.1703.

6-*Neo*·HBr (4). White crystalline solid, yield 54% (3.29 g). ¹H NMR (CDCl₃, 400 MHz, 298 K): δ 7.89 (1H, s, NHCN); 3.46 (2H, t, ³J_{HH} = 5.7 Hz, NCH₂); 3.32 (4H, s, NCH₂C(CH₃)₃); 2.12 (2H, q, ³J_{HH} = 5.2 Hz, NCH₂CH₂); 0.94 (18H, s, NCH₂C(CH₃)₃). ¹³C{¹H} NMR (CDCl₃, 125 MHz, 298 K): δ 156.2 (s, NHCN); 66.7 (s, NCH₂C(CH₃)₃); 46.6 (s, NCH₂); 27.3 (s, NCH₂C(CH₃)₃); 19.3 (s, NCH₂CH₂). MS (ESI): *m/z* 225.2331 (M⁺ – Br) – C₁₄H₂₉N₂ requires 225.2334.

7-*i*Pr·HI (5). White crystalline solid, yield 65% (4.03 g). ¹H NMR (CDCl₃, 400 MHz, 298 K): δ 7.92 (1H, s, NHCN); 3.96 (2H, m, NCH(CH₃)₂); 3.65 (4H, t, ³J_{HH} = 5.8 Hz, NCH₂); 2.04 (4H, q, ³J_{HH} = 5.1 Hz, NCH₂CH₂); 1.29 (12H, d, ³J_{HH} = 6.7 Hz, NCH(CH₃)₂). ¹³C{¹H} NMR (CDCl₃, 125 MHz, 298 K): δ 155.6 (s, NHCN); 58.0 (s, NCH(CH₃)₂); 42.9 (s, NCH₂); 24.4 (s, NCH₂CH₂); 19.2 (s, NCH(CH₃)₂). MS (ESI): *m/z* 183.1864 (M⁺ – I) – C₁₁H₂₃N₂ requires 183.1861.

7-*Neo*·HI (6). White crystalline solid, yield 58% (4.23 g). ¹H NMR (CDCl₃, 400 MHz, 298 K): δ 8.49 (1H, s, NHCN); 3.80 (4H, t, ³J_{HH} = 5.8 Hz, NCH₂); 3.51 (4H, s, NCH₂C(CH₃)₃); 2.15 (4H, q, ³J_{HH} = 4.9 Hz, NCH₂CH₂); 0.99 (18H, s, NCH₂C(CH₃)₃). ¹³C{¹H} NMR (CDCl₃, 125 MHz, 298 K): δ 160.4 (s, NHCN); 69.3 (s, NCH₂C(CH₃)₃); 53.2 (s, NCH₂); 27.2 (s, NCH₂C(CH₃)₃); 25.1 (s, NCH₂CH₂). MS (ESI): *m/z* 239.2487 (M⁺ – I) – C₁₅H₃₁N₂ requires 239.2484.

General procedure for synthesis of [Rh(NHC)(COD)Cl] complexes

A flame dried Schlenk was loaded with the desired NHC·HX salt (0.15 mmol) and dried under vacuum for *ca.* 30 min prior to the addition of dry, degassed THF (10 ml) and KHDMS (0.21 mmol). The solution was stirred for 30 min at ambient temperature and transferred *via* an oven dried filter cannula to a stirred THF (5 ml) solution of [Rh(COD)Cl]₂ (0.075 mmol). The orange solution turned bright yellow immediately upon addition of the free carbene solution. The reaction mixture was allowed to stir for 1 h at ambient temperature before the THF was removed under vacuum and the resultant yellow residue triturated with *n*-pentane to furnish the title compounds as microcrystalline yellow solids.

General procedure for synthesis of [Ir(NHC)(COD)Cl] complexes

A flame dried schlenk was loaded with the desired NHC-HX salt (0.15 mmol); and dried under vacuum for 30 min prior to the addition of dry, degassed THF (10 ml) and KHDMS (0.21 mmol). The solution was stirred at ambient temperature for 30 min and transferred *via* oven dried filter cannula to a stirred THF (5 ml) solution of [Ir(COD)Cl]₂ (0.075 mmol). The bright yellow solution darkened immediately upon addition of the free carbene solution. The reaction mixture was allowed to stir for 1 h at ambient temperature before the THF was removed under vacuum and the resultant yellow/brown oil triturated with *n*-pentane furnishing a brown solid. The isolated solid was further purified *via* flash column chromatography (silica/DCM) and eluted as a yellow band in the first fraction, the eluent was reduced *in vacuo* to afford the title compounds as bright yellow microcrystalline solids.

[Rh(6-*i*Pr)(COD)Cl]¹⁴ (7). Yellow microcrystalline solid, yield 88% (54.7 mg). The physical data obtained was found to be in line with the previously reported complex of Buchmeiser.

[Ir(6-*i*Pr)(COD)Cl] (8). Yellow microcrystalline solid, yield 79% (59.8 mg). ¹H NMR (CDCl₃, 400 MHz, 298 K): δ 6.24 (2H, m, NCH(CH₃)₂), 4.84 (2H, m, CH_{COD}), 3.93 (2H, m, CH_{COD}), 3.22 (4H, t, ³J_{HH} = 5.8 Hz, NCH₂), 2.91 (4H, m, CH_{2 COD}), 1.98 (4H, m, CH_{2 COD}), 1.41 (2H, q, ³J_{HH} = 5.5 Hz, NCH₂CH₂), 1.25 (12H, d, ³J_{HH} = 6.8 Hz, NCH(CH₃)₂). ¹³C{¹H} NMR (CDCl₃, 125 MHz, 298 K): δ (NCN) not observed, 96.1 (s, CH_{COD}), 74.9 (s, CH_{COD}), 58.2 (s, NCH₂), 40.3 (s, NCH(CH₃)₂), 32.6 (s, CH_{2 COD}), 29.5 (s, CH_{2 COD}), 22.5 (s, NCH₂CH₂), 19.4 (s, NCH(CH₃)₂). MS (ES) *m/z*: 503.1932 (M⁺ + H) - C₁₈H₃₃N₂IrCl requires 503.1932.

[Rh(6-Neo)(COD)Cl] (9). Yellow microcrystalline solid, yield 71% (50.1 mg). ¹H NMR (CDCl₃, 400 MHz, 298 K): δ 5.59 (2H, d, ²J_{HH} = 15.4 Hz, NCH₂C(CH₃)₃), 4.78 (2H, m, CH_{COD}), 3.39 (2H, d, ²J_{HH} = 15.5 Hz, NCH₂C(CH₃)₃), 3.15 (2H, t, ³J_{HH} = 5.8 Hz, NCH₂), 3.05 (2H, t, ³J_{HH} = 5.8 Hz, NCH₂), 2.89 (2H, m, CH_{COD}), 2.27 (4H, m, CH_{2 COD}), 1.87 (2H, q, ³J_{HH} = 5.1 Hz, NCH₂CH₂), 1.79 (4H, m, CH_{2 COD}), 1.06 (18H, s, NCH₂C(CH₃)₃). ¹³C{¹H} NMR (CDCl₃, 125 MHz, 298 K): δ 208.0 (d, ¹J_{CRh} = 47.5 Hz, NCN), 94.2 (d, ¹J_{CRh} = 6.3 Hz, CH_{COD}), 69.7 (s, NCH₂C(CH₃)₃), 68.9 (d, ¹J_{CRh} = 15 Hz, CH_{COD}), 45.9 (s, NCH₂), 31.6 (s, CH_{2 COD}), 28.8 (s, NCH₂C(CH₃)₃), 28.0 (s, CH_{2 COD}), 20.6 (s, NCH₂CH₂). MS (ESI): *m/z* 435.2289 (M⁺ - Cl) - C₂₂H₄₀N₂Rh requires 435.2257.

[Ir(6-Neo)(COD)Cl] (10). Yellow microcrystalline solid, yield 91% (76.5 mg). ¹H NMR (CDCl₃, 400 MHz, 298 K): δ 5.38 (2H, d, ²J_{HH} = 15.5 Hz, NCH₂C(CH₃)₃), 4.33 (2H, m, CH_{COD}), 3.21 (2H, t, ³J_{HH} = 5.8 Hz, NCH₂), 3.14 (2H, d, ²J_{HH} = 15.3 Hz, NCH₂C(CH₃)₃), 3.05 (2H, t, ³J_{HH} = 5.8 Hz, NCH₂), 2.51 (2H, m, CH_{COD}), 2.07 (4H, m, CH_{2 COD}), 1.55 (4H, m, CH_{2 COD}), 1.43 (2H, q, ³J_{HH} = 5.1 Hz, NCH₂CH₂), 1.02 (18H, s, NCH₂C(CH₃)₃). ¹³C{¹H} NMR (CDCl₃, 125 MHz, 298 K): δ 202.2 (s, NCN), 78.9 (s, CH_{COD}), 68.9 (s, NCH₂C(CH₃)₃), 52.5 (s, CH_{COD}), 46.8 (s, NCH₂), 32.3 (s, CH_{2 COD}), 31.4 (s, CH_{2 COD}), 28.6 (s, NCH₂C(CH₃)₃), 20.9 (s, NCH₂CH₂). MS (ESI): *m/z* 564.3036 (M⁺ - Cl +

MeCN) - C₂₄H₄₃N₃Ir requires 564.3038. Anal. Calcd for C₂₃H₄₀N₂IrCl: C, 47.17; H, 7.20; N, 5.00. Found: C, 47.19; H, 6.94; N, 4.61.

[Rh(7-*i*Pr)(COD)Cl] (11). Yellow microcrystalline solid, yield 69% (44.3 mg). ¹H NMR (CDCl₃, 400 MHz, 298 K): δ 6.31 (2H, m, NCH(CH₃)₂), 4.93 (2H, m, CH_{COD}), 3.42 (2H, m, CH_{COD}); 3.31 (2H, t, ³J_{HH} = 5.8 Hz, NCH₂), 3.26 (2H, t, ³J_{HH} = 5.9 Hz, NCH₂), 2.19 (4H, m, CH_{2 COD}), 1.80 (4H, m, CH_{2 COD}), 1.58 (4H, q, ³J_{HH} = 5.0 Hz, NCH₂CH₂), 1.26 (12H, d, ³J_{HH} = 5.8 Hz, NCH(CH₃)₂). ¹³C{¹H} NMR (CDCl₃, 125 MHz, 298 K): δ (NCN) not observed, 92.3 (d, ¹J_{CRh} = 6.3 Hz, CH_{COD}), 70.7 (d, ¹J_{CRh} = 13.7 Hz, CH_{COD}), 56.7 (s, NCH₂), 41.4 (s, NCH(CH₃)₂), 30.9 (s, CH_{2 COD}), 28.5 (s, CH_{2 COD}), 24.9 (s, NCH₂CH₂), 20.1 (s, NCH(CH₃)₂). MS (ESI): *m/z* 393.1778 (M⁺ - Cl) - C₁₉H₃₄N₃Rh requires 393.1777.

[Ir(7-*i*Pr)(COD)Cl] (12). Yellow microcrystalline solid, yield 75% (58.3 mg). ¹H NMR (CDCl₃, 400 MHz, 298 K): δ 6.09 (2H, m, NCH(CH₃)₂), 4.28 (2H, m, CH_{COD}), 3.40 (2H, t, ³J_{HH} = 5.9 Hz, NCH₂), 3.21 (2H, t, ³J_{HH} = 5.9 Hz, NCH₂), 2.88 (2H, m, CH_{COD}), 2.08 (4H, m, CH_{2 COD}), 1.79 (4H, m, CH_{2 COD}), 1.56 (4H, q, ³J_{HH} = 4.9 Hz, NCH₂CH₂), 1.25 (12H, d, ³J_{HH} = 5.8 Hz, NCH(CH₃)₂). ¹³C{¹H} NMR (CDCl₃, 125 MHz, 298 K): δ 209.1 (s, NCN), 78.9 (s, CH_{COD}), 56.8 (s, CH_{COD}), 52.4 (s, NCH₂), 42.1 (s, NCH(CH₃)₂), 32.3 (s, CH_{2 COD}), 28.4 (s, CH_{2 COD}), 24.9 (s, NCH₂CH₂), 20.2 (s, NCH(CH₃)₂). MS (ESI): *m/z* 522.2589 (M⁺ - Cl + MeCN) - C₂₁H₃₇N₃Ir requires 522.2594.

[Rh(7-Neo)(COD)Cl] (13). Yellow microcrystalline solid, yield 83% (60.3 mg). ¹H NMR (CDCl₃, 400 MHz, 298 K): δ 4.82 (2H, d, ²J_{HH} = 15.3 Hz, NCH₂C(CH₃)₃), 4.56 (2H, m, CH_{COD}), 3.37 (2H, d, ²J_{HH} = 15.4 Hz, NCH₂C(CH₃)₃), 3.19 (2H, m, CH_{COD}), 2.25 (4H, t, ³J_{HH} = 5.8 Hz, NCH₂), 1.79 (4H, m, CH_{2 COD}), 1.53 (4H, m, CH_{2 COD}), 1.04 (18H, s, NCH₂C(CH₃)₃), 0.37 (4H, q, ³J_{HH} = 5.6 Hz, NCH₂CH₂). ¹³C{¹H} NMR (CDCl₃, 125 MHz, 298 K): δ (NCN) not observed, 96.3 (d, ¹J_{CRh} = 6.3 Hz, CH_{COD}), 72.1 (s, NCH₂C(CH₃)₃), 66.6 (d, ¹J_{CRh} = 15 Hz, CH_{COD}), 55.7 (s, NCH₂), 31.9 (s, CH_{2 COD}), 28.1 (s, NCH₂C(CH₃)₃), 27.0 (s, CH_{2 COD}), 23.5 (s, NCH₂CH₂). MS (ESI): *m/z* 449.2403 (M⁺ - Cl) - C₂₃H₄₂N₂Rh requires 449.2396.

[Ir(7-Neo)(COD)Cl] (14). Yellow microcrystalline solid, yield 76% (65.5 mg). ¹H NMR (CDCl₃, 400 MHz, 298 K): δ 4.41 (2H, d, ²J_{HH} = 15.4 Hz, NCH₂C(CH₃)₃), 4.23 (2H, m, CH_{COD}), 3.47 (2H, m, CH_{COD}), 3.26 (4H, t, ³J_{HH} = 5.9 Hz, NCH₂), 2.92 (2H, d, ²J_{HH} = 15.6 Hz, NCH₂C(CH₃)₃), 2.10 (4H, m, CH_{2 COD}), 1.58 (4H, m, CH_{2 COD}), 1.47 (4H, q, ³J_{HH} = 5.0 Hz, NCH₂CH₂), 1.01 (18H, s, NCH₂C(CH₃)₃). ¹³C{¹H} NMR (CDCl₃, 125 MHz, 298 K): δ 221.2 (s, NCN), 81.2 (s, CH_{COD}), 71.7 (s, NCH₂C(CH₃)₃), 56.2 (s, CH_{COD}), 50.4 (s, NCH₂), 32.1 (s, CH_{2 COD}), 28.3 (s, CH_{2 COD}), 28.1 (s, NCH₂C(CH₃)₃), 25.4 (s, NCH₂CH₂). MS (ESI): *m/z* 580.3243 (M⁺ - Cl + MeCN) - C₂₅H₄₅N₃Ir requires 580.3223. Anal. Calcd for C₂₄H₄₂N₂IrCl: C, 48.10; H, 7.37; N, 4.88. Found: C, 48.39; H, 7.46; N, 4.48.

General procedure for synthesis of [Rh/Ir(NHC)(CO)₂Cl] complexes

A 50 ml round bottom flask was loaded with the corresponding [Rh/Ir(NHC)(CO)₂Cl] complex and dissolved in DCM

(10 ml) followed by CO_(g) (1 atm) bubbled through the solution for 20 min where upon the yellow solution lightened. The solution was reduced *in vacuo* to afford a yellow residue which was triturated with *n*-pentane to yield the corresponding [Rh/Ir(NHC)(CO)₂Cl] complex as a pale yellow microcrystalline solid.

[Rh(6-*i*Pr)(CO)₂Cl] (15). Pale yellow microcrystalline solid, yield 88% (15.4 mg). The physical data obtained was found to be in line with the previously reported complex of Buchmeiser.

[Ir(6-*i*Pr)(CO)₂Cl] (16). Pale yellow microcrystalline solid, yield 86% (15.5 mg). ¹H NMR (CDCl₃, 400 MHz, 298 K): δ 5.84 (2H, m, NCH(CH₃)₂), 3.21 (4H, t, ³J_{HH} = 5.8 Hz, NCH₂), 2.34 (2H, q, ³J_{HH} = 5.4 Hz, NCH₂CH₂), 1.54 (12 H, d, ³J_{HH} = 5.9 Hz, NCH(CH₃)₂). ¹³C{¹H} NMR (CD₃CN, 125 MHz, 298 K): δ 203.6 (s, NCN), 189.4 (s, CO), 181.4 (s, CO), 56.2 (s, NCH(CH₃)₂), 41.8 (s, NCH₂), 23.6 (s, NCH(CH₃)₂), 19.9 (s, NCH(CH₃)₂). FTIR: 1982 (ν(CO I)), 2062 (ν(CO II)).

[Rh(6-Neo)(CO)₂Cl] (17). Pale yellow microcrystalline solid, yield 97% (17.2 mg). ¹H NMR (CDCl₃, 400 MHz, 298 K): δ 4.72 (2H, d, ²J_{HH} = 15.3 Hz, NCH₂C(CH₃)₃), 3.16 (2H, t, ³J_{HH} = 5.9 Hz, NCH₂), 3.12 (2H, t, ³J_{HH} = 5.9 Hz, NCH₂), 3.07 (2H, d, ²J_{HH} = 15.4 Hz, NCH₂C(CH₃)₃), 1.85 (2H, q, ³J_{HH} = 5.0 Hz, NCH₂CH₂), 0.99 (18H, s, NCH₂C(CH₃)₃). ¹³C{¹H} NMR (CDCl₃, 125 MHz, 298 K): δ 199.4 (d, ¹J_{RhC} = 39.1 Hz, NCN), 185.0 (d, ¹J_{RhC} = 53.7 Hz, CO), 183.7 (d, ¹J_{RhC} = 77.5 Hz, CO), 70.7 (s, NCH₂C(CH₃)₃), 47.0 (s, NCH₂), 32.2 (s, NCH₂C(CH₃)₃), 19.4 (s, NCH₂CH₂). MS (ESI): *m/z* 424.1489 (M⁺ – Cl + MeCN) – C₁₈H₃₁N₃O₂Rh requires 424.1471. FTIR: 1989 (ν(CO I)), 2068 (ν(CO II)).

[Ir(6-Neo)(CO)₂Cl] (18). Pale yellow microcrystalline solid, yield 89% (16.1 mg). ¹H NMR (CDCl₃, 400 MHz, 298 K): δ 4.84 (2H, d, ²J_{HH} = 15.4 Hz, NCH₂C(CH₃)₃), 3.16 (2H, t, ³J_{HH} = 5.8 Hz, NCH₂), 3.12 (2H, t, ³J_{HH} = 5.8 Hz, NCH₂), 3.04 (2H, d, ²J_{HH} = 15.4 Hz, NCH₂C(CH₃)₃), 1.91 (2H, q, ³J_{HH} = 4.9 Hz, NCH₂CH₂), 0.99 (18H, s, NCH₂C(CH₃)₃). ¹³C{¹H} NMR (CDCl₃, 125 MHz, 298 K): δ 195.1 (s, NCN), 179.9 (s, CO), 168.6 (s, CO), 70.2 (s, NCH₂C(CH₃)₃), 47.6 (s, NCH₂), 28.1 (s, NCH₂C(CH₃)₃), 19.3 (s, NCH₂CH₂). MS (ESI): *m/z* 514.2031 (M⁺ – Cl + MeCN) – C₁₈H₃₁N₃O₂Ir requires 514.2046. FTIR: 1989 (ν(CO I)), 2068 (ν(CO II)).

[Rh(7-*i*Pr)(CO)₂Cl] (19). Pale yellow microcrystalline solid, yield, 94% (16.5 mg). ¹H NMR (CDCl₃, 400 MHz, 298 K): δ 5.54 (2H, m, NCH(CH₃)₂), 3.39 (4H, t, ³J_{HH} = 5.8 Hz, NCH₂), 2.12 (4H, q, ³J_{HH} = 5.5 Hz, NCH₂CH₂), 1.51 (12H, d, ³J_{HH} = 5.8 Hz, NCH(CH₃)₂). ¹³C{¹H} NMR (CDCl₃, 125 MHz, 298 K): δ (NCN) not observed, 186.3 (d, ¹J_{RhC} = 54.2 Hz, CO), 183.4 (d, ¹J_{RhC} = 77.6 Hz, CO), 57.8 (s, NCH₂), 41.8 (s, NCH(CH₃)₂), 28.1 (s, NCH(CH₃)₂), 18.2 (s, NCH₂CH₂). FTIR: 1988 (ν(CO I)), 2060 (ν(CO II)).

[Ir(7-*i*Pr)(CO)₂Cl] (20). Pale yellow microcrystalline solid, yield 97% (17.5 mg). ¹H NMR (CDCl₃, 400 MHz, 298 K): δ 5.53 (2H, m, NCH(CH₃)₂), 3.36 (4H, t, ³J_{HH} = 5.8 Hz, NCH₂), 1.55 (4H, q, ³J_{HH} = 5.5 Hz, NCH₂CH₂), 1.18 (12H, d, ³J_{HH} = 5.9 Hz, NCH(CH₃)₂). ¹³C{¹H} NMR (CDCl₃, 125 MHz, 298 K): δ (NCN) not observed, 179.9 (s, CO), 165.3 (s, CO), 56.7 (s, NCH₂), 41.5 (s, NCH(CH₃)₂), 27.6 (s, NCH(CH₃)₂), 17.6 (s, NCH₂CH₂). MS

(ESI): *m/z* 460.1568 (M⁺ – Cl + MeCN) – C₁₄H₂₅N₃O₂Ir requires 460.1576. FTIR: 1981 (ν(CO I)), 2056 (ν(CO II)).

[Rh(7-Neo)(CO)₂Cl] (21). Pale yellow microcrystalline solid, yield 93% (16.6 mg). ¹H NMR (CDCl₃, 400 MHz, 298 K): δ 4.22 (2H, d, ²J_{HH} = 15.4 Hz, NCH₂C(CH₃)₃), 3.46 (2H, d, ²J_{HH} = 15.4 Hz, NCH₂C(CH₃)₃), 2.29 (4H, t, ³J_{HH} = 5.9 Hz, NCH₂), 1.23 (4H, q, ³J_{HH} = 5.5 Hz, NCH₂CH₂), 0.99 (18H, s, NCH₂C(CH₃)₃). ¹³C{¹H} NMR (CDCl₃, 125 MHz, 298 K): δ (NCN) not observed, 188.5 (d, ¹J_{RhC} = 55.1 Hz, CO), 181.5 (d, ¹J_{RhC} = 74.2 Hz, CO), 71.6 (s, NCH₂C(CH₃)₂), 54.2 (s, NCH₂), 29.7 (s, NCH₂C(CH₃)₃), 25.8 (s, NCH₂CH₂). MS (ESI): *m/z* 426.1622 (M⁺ – Cl + MeCN) – C₁₈H₃₃N₃O₂Rh requires 426.1628. FTIR: 1972 (ν(CO I)), 2056 (ν(CO II)).

[Ir(7-Neo)(CO)₂Cl] (22). Pale yellow microcrystalline solid, yield 78% (14.2 mg). ¹H NMR (CDCl₃, 400 MHz, 298 K): δ 4.27 (2H, d, ²J_{HH} = 15.2 Hz, NCH₂C(CH₃)₃), 3.51 (2H, t, ³J_{HH} = 5.8 Hz, NCH₂), 3.42 (2H, t, ³J_{HH} = 5.8 Hz, NCH₂), 2.76 (2H, d, ²J_{HH} = 15.2 Hz, NCH₂C(CH₃)₃), 1.88 (2H, q, ³J_{HH} = 5.6 Hz, NCH₂CH₂), 1.73 (2H, q, ³J_{HH} = 5.6 Hz, NCH₂CH₂), 0.98 (18H, s, NCH₂C(CH₃)₃). ¹³C{¹H} NMR (CDCl₃, 125 MHz, 298 K): δ 179.7 (s, NCN), 167.8 (s, CO), 155.7 (s, CO), 72.9 (s, NCH₂C(CH₃)₃), 56.9 (s, NCH₂), 27.5 (s, NCH₂C(CH₃)₃), 24.5 (s, NCH₂CH₂). MS (ESI): *m/z* 526.2170 (M⁺ – Cl + MeCN) – C₁₉H₃₃N₃O₂Ir requires 526.2179. FTIR: 1972 (ν(CO I)), 2054 (ν(CO II)).

General hydrogenation procedure

A 250 ml Parr autoclave equipped with a stirrer bar was loaded with ethanol (20 ml), decane (1 mmol, internal standard), the desired substrate (1 mmol) and the pre-catalyst stock solution (THF). This solution was degassed with nitrogen for *ca.* 5 minutes prior to the sealing to the vessel and purging with molecular hydrogen. The reaction was stirred at ambient temperature for 1 h prior to the venting of the hydrogen and subsequent analysis of the reaction mixture by GCMS. Samples were prepared by the dilution of a 0.3 ml sample with 2 ml HPLC DCM and the elution through a small silica column. Program for analysis: initial temperature at 40 °C, held for 2.5 minutes, ramp 5 °C per minute next 150 °C, ramp 10 °C per minute next 220 °C, held for 10 minutes. The temperature of the injector and detector were maintained at 240 °C.

Identification hydrogenation products

All products were identified through GCMS analysis or ¹H NMR and were found to be in line with previously reported data.

Acknowledgements

We would like to acknowledge the EPSRC and the Cardiff Catalysis Institute (CCI) for JJD's PhD studentship and Johnson Matthey for the generous loan of rhodium and iridium salts.

Notes and references

- 1 For reviews see: (a) F. E. Hahn and M. C. Jahnke, *Angew. Chem., Int. Ed.*, 2008, **47**, 3122; (b) W. A. Herrmann, *Angew. Chem., Int. Ed.*, 2002, **41**, 1290; (c) T. Dröge and F. Glorius, *Angew. Chem., Int. Ed.*, 2010, **49**, 6940; (d) E. A. B. Kantchev, C. J. O'Brien and M. G. Organ, *Angew. Chem., Int. Ed.*, 2007, **46**, 2768.
- 2 (a) D. G. Gusev, *Organometallics*, 2009, **28**, 6458; (b) R. Tonner and G. Frenking, *Organometallics*, 2009, **28**, 3901.
- 3 For a review see: S. Diez-Gonzalez, N. Marion and S. P. Nolan, *Chem. Rev.*, 2009, **109**, 3612.
- 4 (a) M. Iglesias, D. J. Beetstra, J. C. Knight, L. Ooi, A. Stasch, S. Coles, L. Male, M. B. Hursthouse, K. J. Cavell, A. Dervisi and I. A. Fallis, *Organometallics*, 2008, **27**, 3279; (b) W. Y. Lu, K. J. Cavell, J. S. Wixey and B. Kariuki, *Organometallics*, 2011, **30**, 5649.
- 5 (a) M. Iglesias, D. J. Beetstra, J. C. Knight, L. L. Ooi, A. Stasch, S. Coles, L. Male, M. B. Hursthouse, K. J. Cavell, A. Dervisi and I. A. Fallis, *Organometallics*, 2008, **27**, 3279; (b) E. L. Kolychev, I. A. Portnyagin, V. V. Shuntikov, V. N. Khrustalev and M. S. Nechaev, *J. Organomet. Chem.*, 2009, **694**, 2454; (c) W. A. Herrmann, S. K. Schneider, K. Ofele, M. Sakamoto and E. Herdtweck, *J. Organomet. Chem.*, 2004, **689**, 2441.
- 6 (a) M. Iglesias, D. J. Beetstra, A. Stasch, P. N. Horton, M. B. Hursthouse, S. J. Coles, K. J. Cavell, A. Dervisi and I. A. Fallis, *Organometallics*, 2007, **26**, 4800; (b) A. Binobaid, M. Iglesias, D. J. Beetstra, B. Kariuki, A. Dervisi, I. A. Fallis and K. J. Cavell, *Dalton Trans.*, 2009, 7099; (c) P. D. Newman, K. J. Cavell, A. J. Hallett and B. M. Kariuki, *Dalton Trans.*, 2011, **40**, 8807; (d) P. Bazinet, G. P. A. Yap and D. S. Richeson, *J. Am. Chem. Soc.*, 2003, **125**, 13314; (e) C. C. Scarborough, I. A. Guzei and S. S. Stahl, *Dalton Trans.*, 2009, 2284; (f) M. Iglesias, D. J. Beetstra, B. Kariuki, K. J. Cavell, A. Dervisi and I. A. Fallis, *Eur. J. Inorg. Chem.*, 2009, 1913; (g) D. Mercan, E. Çetinkaya and B. Çetinkaya, *J. Organomet. Chem.*, 2011, **696**, 1359; (h) I. Özdemir, S. Demir, B. Çetinkaya and E. Çetinkaya, *J. Organomet. Chem.*, 2005, **690**, 5849; (i) N. Imlinger, K. Wurst and M. R. Buchmeiser, *J. Organomet. Chem.*, 2005, **690**, 4433; (j) C. Segarra, E. Mas-Marzá, J. P. Lowe, M. F. Mahon, R. C. Poulten and M. K. Whittlesey, *Organometallics*, DOI: 10.1021/om300984v.
- 7 A. Binobaid, M. Iglesias, D. Beetstra, A. Dervisi, I. Fallis and K. J. Cavell, *Eur. J. Inorg. Chem.*, 2010, **2010**, 5426.
- 8 (a) J. J. Dunsford, K. J. Cavell and B. Kariuki, *J. Organomet. Chem.*, 2011, **696**, 188; (b) P. D. Newman, K. J. Cavell and B. M. Kariuki, *Dalton Trans.*, 2012, **41**, 12395.
- 9 (a) C. C. Scarborough, A. Bergant, G. T. Sazama, I. A. Guzei, L. C. Spencer and S. S. Stahl, *Tetrahedron*, 2009, **65**, 5084; (b) C. C. Scarborough, M. J. W. Grady, I. A. Guzei, B. A. Gandhi, E. E. Bunel and S. S. Stahl, *Angew. Chem., Int. Ed.*, 2005, **44**, 5269; (c) J. J. Dunsford and K. J. Cavell, *Dalton Trans.*, 2011, **40**, 9131; (d) U. Siemeling, C. Färber, C. Bruhn, S. Fürmeier, T. Schulz, M. Kurlmann and S. Tripp, *Eur. J. Inorg. Chem.*, 2012, **9**, 1413; (e) P. Hauwert, J. J. Dunsford, D. S. Tromp, J. J. Weigand, M. Lutz, K. J. Cavell and C. J. Elsevier, *Organometallics*, DOI: 10.1021/om300930w.
- 10 (a) C. J. E. Davies, M. J. Page, C. E. Ellul, M. F. Mahon and M. K. Whittlesey, *Chem. Commun.*, 2010, **46**, 5151; (b) P. D. Newman, K. J. Cavell and B. M. Kariuki, *Organometallics*, 2010, **29**, 2724.
- 11 P. D. Newman, K. J. Cavell and B. M. Kariuki, *Chem. Commun.*, 2012, **48**, 6511.
- 12 (a) T. W. Hudnall, A. G. Tennyson and C. W. Bielawski, *Organometallics*, 2010, **29**, 4569; (b) J. J. Dunsford, K. J. Cavell and B. M. Kariuki, *Organometallics*, 2012, **31**, 4118.
- 13 (a) R. Armstrong, C. Ecott, E. Mas-Marzá, M. J. Page, M. F. Mahon and M. K. Whittlesey, *Organometallics*, 2010, **29**, 991; (b) V. Friese, S. Nag, J. Wang, M.-P. Santoni, A. Rodrigue-Witchel, G. S. Hanan and F. Schaper, *Eur. J. Inorg. Chem.*, 2011, **1**, 39.
- 14 M. Mayr, K. Wurst, K.-H. Ongania and M. R. Buchmeiser, *Chem.-Eur. J.*, 2004, **10**, 1256.
- 15 (a) F. E. Hahn, C. Holtgrewe, T. Pape, M. Martin, E. Sola and L. A. Oro, *Organometallics*, 2005, **24**, 2203; (b) J. R. Miecznikowski and R. H. Crabtree, *Organometallics*, 2004, **23**, 629; (c) R. Corberan and E. Peris, *Organometallics*, 2008, **27**, 1954; (d) R. Corberan, M. Sanau and E. Peris, *Organometallics*, 2007, **26**, 3492; (e) A. Zanardi, E. Peris and J. A. Mata, *New J. Chem.*, 2008, **32**, 120; (f) F. Hanasaka, K.-i. Fujita and R. Yamaguchi, *Organometallics*, 2004, **23**, 1490; (g) J. A. Brown, S. Irvine, A. R. Kennedy, W. J. Kerr, S. Andersson and G. N. Nilsson, *Chem. Commun.*, 2008, 1115.
- 16 M. Albrecht, J. R. Miecznikowski, A. Samuel, J. W. Faller and R. H. Crabtree, *Organometallics*, 2002, **21**, 3596.
- 17 For the original 'click' ring closure protocol see: R. Jazzar, H. Liang, B. Donnadieu and G. Bertrand, *J. Organomet. Chem.*, 2006, **691**, 3201.
- 18 K. Hirano, S. Urban, C. Wang and F. Glorius, *Org. Lett.*, 2009, **11**, 1019.
- 19 K. M. Kuhn and R. H. Grubbs, *Org. Lett.*, 2008, **10**, 2075.
- 20 E. M. Higgins, J. A. Sherwood, A. G. Lindsay, J. Armstrong, R. S. Massey, R. W. Alder and A. C. O'Donoghue, *Chem. Commun.*, 2011, **47**, 1559.
- 21 L. J. Farrugia, *J. Appl. Crystallogr.*, 1997, **30**, 565.
- 22 (a) R. W. Alder, P. R. Allen, M. Murray and A. G. Orpen, *Angew. Chem., Int. Ed.*, 1996, **35**, 1121; (b) R. W. Alder, M. E. Blake, S. Bufali, C. P. Butts, A. G. Orpen, J. Schutz and S. J. Williams, *J. Chem. Soc., Perkin Trans. 1*, 2001, 1586.
- 23 This feature has also been observed in a related silver(I) complex in an earlier report by Stahl and co-workers (see ref. 9a).
- 24 A. Poater, B. Cozenza, A. Correa, S. Giudice, F. Ragone, V. Scarano and L. Cavallo, *Eur. J. Inorg. Chem.*, 2009, 1759.

- Parameters applied for SambVca calculations: 3.50 Å was selected as the value for the sphere radius, 2.00 Å was used as distances for the metal–ligand bond, hydrogen atoms were omitted, and bond radii scaled by 1.17 were used. The above parameters applied are identical to those of all literature examples discussed allowing a direct comparison of calculated values.
- 25 J. Huang, H. J. Schanz, E. D. Stevens and S. P. Nolan, *Organometallics*, 1999, **18**, 2370.
- 26 For a comprehensive review of % V_{bur} values of NHC complexes see: H. Clavier and S. P. Nolan, *Chem. Commun.*, 2010, **46**, 841.
- 27 (a) C. A. Tolman, *Chem. Rev.*, 1977, **77**, 313;
(b) R. A. I. Kelly, H. Clavier, S. Giudice, N. M. Scott, E. D. Stevens, J. Borden, I. Samardjiev, C. D. Hoff, L. Cavallo and S. P. Nolan, *Organometallics*, 2008, **27**, 208.
- 28 D. D. Perrin and W. F. A. Amarego, *Purification of Laboratory Chemicals*, Oxford, Pergamon, 1988.